J. Mountain Res. P-ISSN: 0974-3030, E-ISSN: 2582-5011 DOI: https://doi.org/10.51220/jmr.v19-i2.7
Vol. 19(2), (2024), 53-65

Biological Docking properties of 4-phenyl piperazin-1-ium and Geometry, QTAIM, NBO, NLO, and Vibrational analysis, of 4-phenyl piperazin-1-iumtrifluoroacetate salts : A DFT study

Dubey D.D.[1] • V. N. Mishra[2*] • S. I. Ansari[2] • G. Mishra[1] • S. N. Tiwari[1] • A. Tiwari[1] • A. K. Pandey[1] • A. K. Dwivedi[3]

[1]*Department of Physics K S Saket P G College Ayodhya*
[2]*Department of Physics, S.R.M.G.P.C. Lucknow*
[3]*Department of Chemistry, Kisan College Sohsarai , Biharsharif, Nalanda, Patliputra University,Patna*

[*]Corresponding Author Email: vnvictorious@gmail.com

Received: 20.7.2024 Revised: 21.9.2024 Accepted: 24.9.2024

Abstract: The optimised geometry of salt 4-phenyl piperazin-1-ium trifluoroacetate employed through the combination DFT/B3LYP along with basis set of 6-311G(d, p). The Quantum theory of atoms is used to calculate nonbonding performance at a bond critical point (BCP). Vibrational analysis of title salt is carried out on optimized geometry and vibrational assignment is done and also view through gauss view interface. Correlation factor shows that the given method well explained the geometry of studied salt. The Natural bond analysis of studied salt describe the mechanism of hyperpolarizability and charge transfer in salt formation. The Electronic surfaces drown on isodensity surfaces been used to determine electronic properties and chemical reactivity aspect of title salt. The transport properties like Log P and Log S of 4-phenyl piperazine has been established in its pharmaceutical behaviour. The biological properties of 4-phenyl piperazine are enumerated through the online server PASS. The Docking of 4-phenyl piperazine with selected target 5B8U protein been described and viewed through online facility server Swiss dock. The docking calculation and binding affinity in 4-phenyl piperazine with 5B8U protein shows its drug designing ability in future.

Keywords: QTAIM • NBO • NLO • HOMO • LUMO • MESP

Introduction

For better and wider understanding of any molecules is best to know about insights of its quantum chemical aspect which may explore it in a newer dimension which may also produce it in a new computational frame work which may help it in various scaling and simulation analysis by using various incorporated theories and systems. The exchange-correlation function incorporates the Density functional theory a better description about energy. The density functional theory shows a better of description of geometry vibrational analysis, electronic properties, charge transfer through NBO and NLO properties of any chemical system (Pandey et al 2013 and Dwivedi et al 2012).

Therapeutic uses of Piperazine derivatives are employed in microbial infections with bacterial, fungal, and tubercular. Microbial infections are becoming problematic due to the eternal issues of resistance entertained by microbial entity along through antibiotics hereafter has important to design newer anti-infective agents for concerned antimicrobials agents (Kharb et al 2011). Nowadays molecule with heterocyclic nuclei plays an important role in the pharmacological activity of microbial infections (Kharb et al 2011). The Piperazine ring is heterocyclic with two N atoms are hetero atoms having medicinal importance (Kharb et al 2012 and Faist et al 2012). Most Importantly Piperazine derivative is one of the important organic compounds Piperazine contains a very well established stable configuration Geometry. It showed lot of attention due to its wide biological applications e.g. drug designing. It

basically established a support which is been viewed as a core in dynamic materials crosswise a diversity of various therapeutic drugs (Ghorbani et al 2015 and Kulig et al 2007). The piperazine ring has vast and various role like as a therapeutic antimicrobial material, an anti-tubercular drugs material and antipsychotic supplement, an important anticonvulsant agent, a well antidepressant agent, very good anti-inflammatory supplement agents etc. (Pietrzycka et al 2006 and Patel et al 2013).

In molecule, Piperazine is mostly present as target CNS receptors, e.g. adrenergic and dopaminergic (Lopez-Rodriguez et al 2002). In the Piperazine ring due to the presence of two N-atoms which that maintain appropriate pKa, Piperazine acts as a drug candidates (Soskic et al 1998). The two nitrogen sites present in the Piperazine ring encourage the water accessibility which may increase it bio utility during it vital application. The Piperazine ring keeping a balance among pharmacodynamic and pharmacokinetic profiles and also plays a very enthusiastic and wonder element in the discovery of newer drugs. In the drug development process, this is important to design molecules that have a large affinity for its targets and suitable physicochemical properties. The synthesis X-ray crystallographic data of 4-nitrophenylpiperazine with acids (Prasad et al 2023) namely, 4-phenyl piperazin-1-ium trifluoroacetate, an organic acid of piperazine derivative 4- is reported. The optimised geometry of 4-phenyl piperazin-1-ium trifluoroacetate has been established through DFT/B3LYP and 6-311G(d,p) method. The nature of the interaction was studied by using QTAIM analysis NBO and NLO behaviour of a given salt. The biological activity and docking properties of 4-phenyl piperazin-1-ium are also reported. It our firm configuration that this study will definitely provides a brighter path to established new drugs for anti-inflammatory in future. The nonlinear optical behaviour shows that salt 4-phenyl piperazin-1-ium trifluoroacetate better liquid crystal agent in displays.

Computational Details

Initial structure of 4-phenyl piperazin-1-ium trifluoroacetate was constructed and labed through a software package Gauss View 6.0. Designed geometry of 4-phenyl) piperazin-1-ium trifluoroacetate is labelled and iterated without having any symmetry constraints. The entire simulation has been performed on principal of DFT/B3LYP method (Lee et al 1988, Scott et al 1996 and Hohenberg et al.) along with 6-311G(d,p) basis set. All calculations on the title salt have been performed on Gaussian 09 program package (Frisch et al 2009). In general, DFT overestimated calculated frequencies so to compare it all estimation are scaled through a scaling factor 0.963 (Pulay et al 1983). The vibrational frequency assignments were enumerated through GAUSSVIEW'S program (Dennington et al 2016) incorporated with symmetry convention. Numerous studies explained the IR spectra of organic molecules by B3LYP methods along with a 6-311 G(d,p) basis set. The frontier molecular orbital HOMO and LUMO are plotted by GAUSSVIEW'S program.

Geometry Optimization

The chemical formula of title molecule $(C10H14N)^{+}(C2Cl3O2)^{-}$ with Monoclinic, P21/c Crystal system, space group symmetry. The lattice parameters of the title molecule are $a=11.7825A^{0}$, $b=6.6142A^{0}$, $c=20.3271A^{0}$ with $\beta=104.173^{0}$.

The title salt is optimized with help of DFT/ 6-311 G(d,p) method. The minimum energy of title salt is -2341.11 a.u. with no symmetry. The animated optimized geometry of salt shows a piperazine ring forming chair conformation. The phenyl ring attached to the nitrogen of the piperazine ring is shown in Fig-1. The computed angle between the -NCN of piperazine ring 38.67^{0} is well matched with the corresponding observed bond angle. The

DOI: https://doi.org/10.51220/jmr.v19-i2.7

delocalization effect is disturbed in the benzene ring due to the occurrence of electron-donating piperazinyl. The substitution of electron donating on the para position group on the benzene ring causes disturbance of planarity due to this reason C_1-C_5 and C_4-C_3 bonds are slightly elongated however conjugative bonds are slightly shortened. The positional disorder of CF_3 affects the geometries of the COO^- groups.

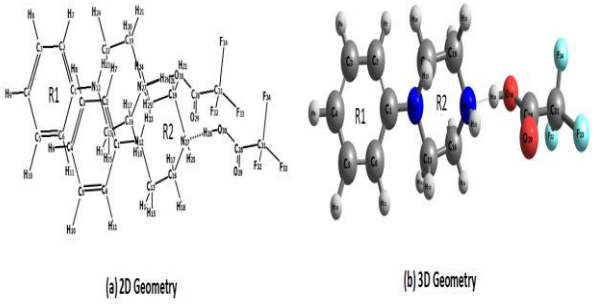

Fig-1 Optimized geometry of 4-(4-nitrophenyl) piperazin-1-ium trifluoroacetate anions (a) 2D (b) 3D geometry

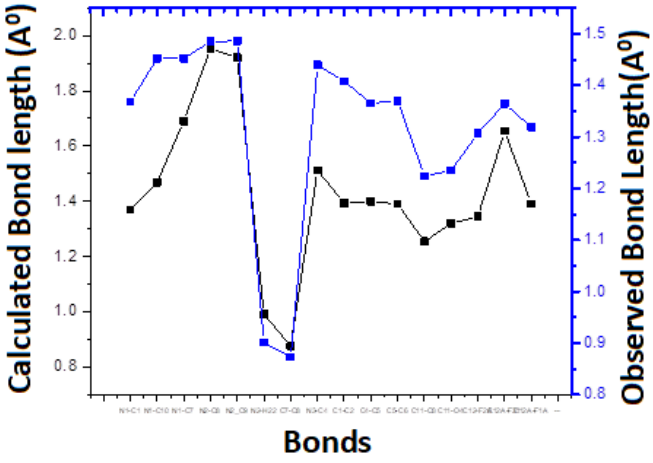

Fig-2 Optimized and Observed Bond length of Title molecule salt

The calculated and observed bond length of the most stable structure of title salt are displayed in Fig-2.The calculated bond length and bond angle are correlated with corresponding observed values and shown in Fig-3(a)&(b). The correlation factor for bond length R^2=0.9787 and bond angle R^2= 0.9886 shows that our computational technique well-explained geometry of the title molecule. Let us check more closely the interaction of 4-phenyl piperazin-1-ium with dichloroacetate by using QTAIM analysis.

QTAIM Analysis: To study inter or intra-molecular interaction of any chemical system QTAIM analysis (Matta et al 2007) is an important method. In QTAIM analysis nature and strength of any chemical system are measured by using some topological parameters at bond critical points (BCP). For any nonbonding interaction (Koch et al 1995) electron density (ρ_{bcp}) should be within the range of 0.002–0.040 a.u., however Laplacian ($\nabla^2\rho_{bcp}$) within the range 0.024–0.139 a.u. By applying this criterion to our system one nonbonding interaction in between O_{30}-H_{27} is recorded. For this interaction charge density ρ_{bcp} is 0.024 a.u., however Laplacian ($\nabla^2\rho_{bcp}$) is 0.114 a.u. The Molecular graphs for nonbonding interaction are presented in Fig-3. The nonbonding interaction nature is

described by Rozas et al. (Rozas et al 2000) criteria. Based on Rozas et al. criteria for H_{26}-O_{30} bond ($\nabla^2\rho_{bcp}>0$ and H(0.0027)>0) are weak electrovalent. The strength of nonbonding interaction is calculated by ΔE_{int}= ½ (V_{BCP}) (Espinosa et al 1998). By using this formula, the strength of nonbonding interaction is 4.995 kcal/mol and lies in weak interactions (E_{int}<5kcal/mol). (Espinosa et al 1998)

The nonbonding interaction in salt is deliberate via Natural bond (NBO) analysis. All possible acceptor molecular orbitals and filled donor molecular orbitals can be carried out using NBO analysis. The lone pair of $Lp(1)O_{30}$/$Lp(3)O_{30}$ with $\sigma^*(N_{26}$-$H_{27})$ stabilized title molecule by 5.08 kcal/mol confirms interaction between O_{30}---H_{27}-N_{26}.

.

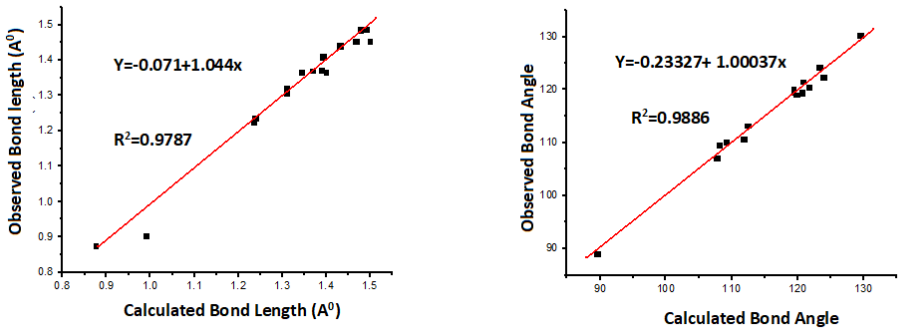

(a) (b)

Fig-3 Graph plotted in between calculated and Observed bond length (a), bond angle (b)

Electronic Properties

The highest occupied molecular orbital (HOMO) and lowest unoccupied molecular orbital (LUMO) plays an significant role in chemical reactivity and termed as frontier molecular orbitals. The HOMO energy level primarily acts as a donor however LUMO acts as an electron acceptor. The energy required in the transition of electrons from HOMO to LUMO orbital is known as the energy gap. The chemical reactivity of any chemical system is determined by less energy required in the transition of electrons from HOMO to LUMO means chemical reactivity is inversely proportional to the band gap. As the energy gap between HOMO to LUMO energy is lesser means much polarization appears in molecules less kinetic stable (Bose et al 2011). The HOMO energy level of the title molecule is at -5.985eV however LUMO is at -0.484 eV and the energy gap 5.501 eV lies within other organic molecules (Bose et al 2011). The energy gap of the title molecule is >5 eV shows that the title molecule is nonreactive. The HOMO and LUMO plot of title are shown in Fig-4. The HOMO is located upon 4-phenyl piperazine however HOMO(MO=72) is distributed over the phenyl ring. The HOMO is LP (3) F34 electron having 99.97 % p character with slightly shifted d (0.03%) character. The LUMO is RY*(1) C1 electron having a mixed character with s (3.39%), p (87.71%), d (8.90%). The transition of electrons from HOMO to LUMO displays electron transfer from piperazine to phenyl ring.

Several global reactivity of the title salt are intended (Table-1) by using a appropriate recipe (Singh et al 2024, Pandey et al 2024 and Pandey et al 2023)

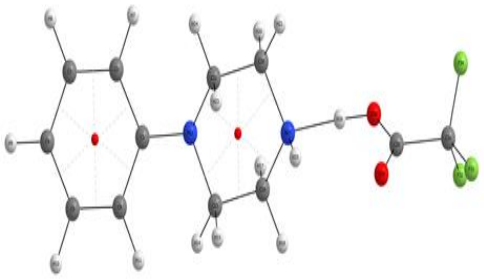

Figure-4 QTAIM picture of interaction of 4-(4-nitrophenyl) piperazin-1-ium cation interacts with trifluoroacetate anions Dotted line represents nonbonding interactions Redpoint (RCP) white point (BCP)

Table-1 Several Electronic reactivity descriptor of title molecule is calculated and listed

Reactivity Index	Values (in eV)
I.P.= $-E_{HOMO}$	0.21997
E.A.= $-E_{LUMO}$	0.01780
$\mu = -\frac{I.P.+E.A.}{2}$	-3.23494
$\chi = \frac{I.P.+E.A.}{2}$	3.23494
$\eta = \frac{I.P.-E.A.}{2}$	2.750594
$S = \frac{1}{\eta}$	0.181779
$\omega = \frac{\chi^2}{2\eta}$	1.902292

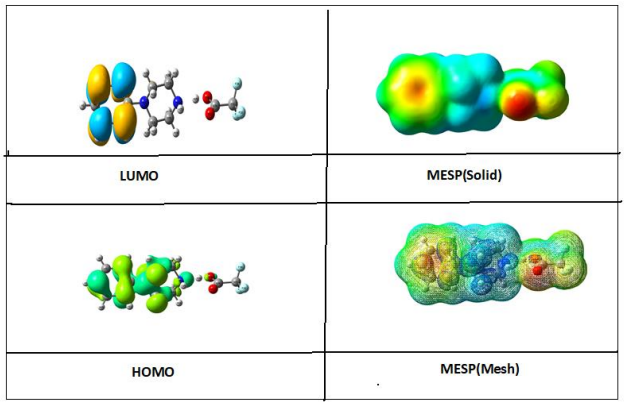

Fig-5 HOMO LUMO MESP(Mesh) MESP (Solid) of 4-(4-nitrophenyl)piperazin-1-ium cation interacts with trifluoroacetate anions

The electrophilicity index (ω) (Lee et al 1989, Parr et al 1999 and Chattaraj et al 2007) is basically shows its stability after acquiring an electronic charge. The electrophilicity index (ω) is related to chemical potential and chemical hardness and is a positive quantity. The electrophilic species capable of acquiring charge form a donor and then the energy required to stabilize the whole chemical system is known as chemical potential. The Chemical potential decides the direction of charge flow and is a negative quantity.

Molecular electrostatic potential (MEP) analysis

The nucleophilic and electrophonic attack charge centre of any chemical system is defined by molecular electrostatic potential (MEP). The correlation between physiochemical property and molecular structure (Padmanabhan et al 2007) is established by the MEP plot. The strength of the electrostatic potential of any molecule is defined according to colour coding e.g. red means negative electrostatic potential; blue means the most positive electrostatic potential and green colour shows zero potential. The electrostatic potential reductions as

blue>green>yellow>orange>red. The MEP plot of the title molecule is shown in Fig-5. The red colour encircled the acetate group and blue over the piperazine ring of the title molecule. The colour coding of the MEP plot shows that the acetate group of the second interacting species trifluoroacetate shows the most electronegative charge centre however piperazine ring shows the most electropositive charge centre. The phenyl ring encircled over yellow colour means inactive centre.

Non Linear Optical (NLO) behaviour of 4-phenyl piperazin-1-iumtrifluoroacetate salts

The nonlinear optical analysis for any chemical structure is defined by several parameters like dipole moment μ, mean polarizability <α>, anisotropy in polarizability (Δα), order parameters and first static hyperpolarizability β. The NLO parameters are computed of 4-phenyl piperazin-1-iumtrifluoroacetatesalts by using appropriate formula (Singh et al., 2024, Pandey et al., 2024 and Pandey et al. 2023).

Table-2 Several nonlinear optical values of salt computed by DFT/6-311G(d,p)

Dipole Moment(μ_{total}) (in debye)		Ist order static hyperpolarizability (β)	
μ_x	5.0335	β_{xxx}	16.1159
μ_y	-0.1938	β_{xxy}	-3.2384
μ_z	-0.1531	β_{xyy}	-22.3535
μ_{tot}	5.0396	β_{yyy}	-0.4518
Polarizability (α) in esu.($\times 10^{-24}$)		β_{xxz}	2.0205
α_{xx}	216.307	β_{xyz}	13.1487
α_{xy}	0.063	β_{yyz}	-1.1534
α_{yy}	141.541	β_{xzz}	-53.9668
α_{xz}	2.341	β_{yzz}	-2.5690
α_{yz}	6.971	β_{zzz}	-5.0300
α_{zz}	103.647	β_{total}(au)	60.6718806
α_{mean} (esu)	153.8317	β_{total}(esu)	524.162578
α_{aniso}	99.29296	MR(a.u.)	57.51766
		S	0.211

* Conversion: for α_{mean}; 1 a.u.= 0.1482×10^{-24}esu, and for β_{total}; 1 a.u. = 8.6393×10^{-33}esu

According to Lorenz-Lorentz (Padmanabhan et al 2007 and Murray et al 1996) molar refractive index of any molecule is calculated with help of given equation

$$MR= 1.33\alpha\pi N$$

In this equation N is the Avogadro number; α is the average polarizability.

The molecular polarizability (α_e) polarizability along x and ordinary polarizibility (α_o) molecular polarizibility along y axis are termed as extraordinary polarizibility and ordinary polarizability respectively, By using these parameters ordered parameter is computed by following

DOI: https://doi.org/10.51220/jmr.v19-i2.7

equation (Verma et al 2005 and Gutsev et al 2012)

$$S=\frac{\alpha_e-\alpha_o}{\alpha_e+\alpha_o}$$

The nonoptical parameters are computed and presented in Table-2. The dipole moment of any chemical structure is depending on its structure and charge distribution. The computed dipole moment of title molecule is 5.04D which is nearly two times dipole moment of water mean title molecule better solvent. The polarity arises due to charge transfer by donor trifluroacetate species.

By application of applied electric field change appears in charge distribution along field is computed by mean polarizability. The computed average polarizability is 153.83 a.u. of title molecule.

The nonlinear optical response by application of applied field is termed as hyperpolarizability. The charge transfer due to application of field mean moment of π electron within molecule is directly related to hyperpolarizability. The hyperpolarizability of any system is third rank 3x3x3 tensor. The Kleinman symmetry component of hyperpolarizability tensor 27 reduced into 10 components (Colthup et al 1990). The intended hyperpolarizability of 4-phenyl piperazin-1-ium trifluoroacetate salts is nearly 59 times of reference molecule Urea. The intended hyperpolarizability of Lithiated Graphene Quantum Dot modulated by Li, Na, are higher than calculated hyperpolarizability of title molecule (Srivastava et al 2021). The intended hyperpolarizability is similar with doping of indigo auxiliary donor, donor and acceptor (Palwasha et al 2021). The NBO analysis shows a number of significant $\pi\rightarrow\pi''$ appears in title molecule. A significant interaction of this type seems amnong $\pi(C_{28}\text{-}C_{29})\rightarrow\pi''(C_{28}\text{-}C_{29})$ which stabilize 4-phenyl piperazin-1-ium trifluoroacetate salts with 3.92kcal/mol. The noteworthy involvement of 18.38 kcal/mol appears due to charge handover from $\pi(C_4\text{-}C5)\rightarrow\pi''(C_1\text{-}C_6)$ which further enhance to 23.62 kcal/mol for $\pi''(C_2\text{-}C_3)$. The strongest contribution of 54.62 kcal/mol appears due to charge allocation from $\pi(C_1\text{-}C_6)\rightarrow\pi''(C_4\text{-}C_5)$. A number of $\pi\rightarrow\pi''$ electron moment is accountable for high nonlinear optical behaviour in 4-phenyl piperazin-1-iumtrifluoroacetate salts.

The 4-phenyl piperazin-1-iumtrifluoroacetate salts is better nonlinear optical response so have a better scope for liquid crystal material in future.

Vibrational analysis

Title molecule having 34 atoms so it covers 3N-5 (97) modes of vibration. Out of 97 modes of vibration N-1 (33) are stretching modes and rest are bending modes. The entire vibrational spectra of title molecule alienated in two portions. The first portion called functional group region which area above 1000 cm^{-1} and second part of spectra called fingerprint region which lies below 1000cm^{-1}. The calculated and scaled frequencies IR along with intensity and modes of vibration listed in above Table-3.

Some particular scaled modes of vibrations are deliberated below.

-C-H modes of vibration

The -CH group present on benzene ring and other portion so -CH stretching modes seems in vibrational investigation. Generally, C-H stretching modes seems in among 3000-3200 cm^{-1}, (Rastogi et al 2002) which is the distinguishing region for identification of the C-H stretching vibration. In present study C-H stretching vibration are calculated at 3200 cm^{-1} to 2925 cm^{-1} for title molecule with significant intensity. A significant polarized mode of vibration appears at 3063 cm^{-1} due to C-H stretching modes in R1 however less intense modes appear at 3200 cm^{-1}. Another intense band seems at 2933 cm^{-1} and 2808 cm^{-1} again owing to C-H stretching modes in R1.

Table- 3 The scaled calculated IR intensity and Assignment of title molecule

SR. No.	Calculated Freq	Scaled Freq	Exp. IR	Assignment
1	3471	3332	4.98	$\upsilon(N_{27}\text{-}H_{25})$
2	3200	3072	8.00	$\upsilon(C\text{-}H)R_1$
3	3191	3063	32.15	$\upsilon(C\text{-}H)R_1$
4	3119	2994	14.61	$\upsilon_{as}(C_{22}\text{-}H_{24})$
5	3101	2977	35.34	$\upsilon_{as}(H_{17}\text{-}C_{16}\text{-}H_{18})+\upsilon_{as}(H_{20}\text{-}C_{19}\text{-}H_{21})$
6	3055	2933	35.63	$\upsilon(H_{17}\text{-}C_{16}\text{-}H_{18})+\upsilon(H_{20}\text{-}C_{19}\text{-}H_{21})$
7	2925	2808	109.28	$\upsilon(C_{22}\text{-}H_{23})+\upsilon(C_{13}\text{-}H_{15})$
8	2478	2379	3638.15	$\upsilon(O_{30}\text{-}H_{26})$
9	1817	1745	309.33	$\beta_{in}(H_{26}\text{-}O_30\text{-}C_{28}\text{-}C_{31)+}\upsilon(_{28}\text{-}HO_{29})$
10	1650	1584	78.77	$\beta_{in}(C\text{-}H)R1+\upsilon(CC)R1$
11	1624	1559	10.33	$\beta_{in}(C\text{-}H)R1+\upsilon(CC)R1$
12	1564	1501	21.86	$\beta_{in}(H_{26}\text{-}O_{30}, N_{27}\text{-}H_{25})$
13	1537	1476	87.54	$\beta_{in}((C\text{-}H)R1,H_{15}\text{-}C_{13}\text{-}H_{14})+\upsilon(C_1\text{-}N_{22})$
14	1503	1443	20.31	□$(CH_2)R_2$
15	1502	1442	13.13	□$(CH_2)R_2$
16	1426	1369	39.67	$\Phi(CH_2)R_2$
17	1424	1367	17.23	$\Phi(CH_2)R_2$
18	1388	1332	83.61	$\upsilon_{as}(O_{30}\text{-}C_{28}\text{-}C_{31})+\beta_{in}(H_{26}\text{-}O_{30})+\beta_{out}(C\text{-}H)R_2$
19	1294	1242	32.76	$\Omega(CH_2)R_2+1+\upsilon(CC)R_1$
20	1260	1210	179.84	$\beta_{out}(C\text{-}H)R_2+\beta_{in}(C\text{-}H)R_1+\upsilon(N_{12}\text{-}C_1)$
21	1218	1169	376.80	$\beta_{out}(F_{34}\text{-}C_{31}\text{-}F_{32})+\upsilon(C_{31\text{-}F33,}\ C_{28}\text{-}O_{30})$
22	1185	1137	345.25	$\beta_{out}(F_{34}\text{-}C_{31}\text{-}F_{32}\text{-}F_{33})+\upsilon(C_{28}\text{-}O_{30})+\tau(C\text{-}H)R_2$
23	1045	1003	11.65	$\beta_{out}(CCC)R_2+\tau(C\text{-}H_2)R_2$
24	941	903	154.57	$\beta_{in}(C\text{-}H)R_1+\beta_{in}\ (CC)R_1$
25	932	895	125.58	$\beta_{in}(C\text{-}H)R_1+\beta_{in}\ (CC)R_1$
26	789	757	15.37	$\beta_{out}(COOH)+\beta out(CF_3)$
27	773	742	44.78	$\beta_{out}(CCC)R_1+\beta out(CH)R_1$
28	717	688	18,67	□$(CF_3)+$□(COOH)
29	708	680	36.09	$\beta_{out}(CCC)R_1+\beta_{out}(CH)R_2$
30	538	516	15.77	$\beta_{out}(CCC)R1+\beta_{out}(CH)R_2$

Note:- ν-Stretching, ν_{as} –Asymmetric stretching, β_{in} - plane angle bending, β_{out} - out-of-plane bending, τ – torsion, □- Sisoring Ω-Twisting Φ-Wagging.

In middle region of spectra some bending modes appears incorporate with –C=C stretching modes of vibration. In in plane -CH bending modes appears at 1817cm^{-1}. The alteration in structure straight connected with modification in the incidence and in H-X stretching important change in wave numbers and also variation in intensity seems. The extent in change of wave numbers H–X stretching is vital limitations to regulate strength of intermolecular interaction. One important think noticed that change in H-X stretching wave numbers is incorporated with interaction energy. At lower frequency region CH in-plane bending modes mixing with several other modes appears at 1650 cm^{-1}, 1559 cm^{-1} due to in-plane -CH bending however at 1045 cm^{-1}, 773 cm^{-1} due to out of plane bending modes appears

Methylene(-CH2) Vibration

The movement of CH_2 group due to Inner coordinates procedure six modes of vibrations like symmetric and antisymmetric rocking, wagging, scissoring, twisting modes are reported. Moreover, due to weaker bond strength symmetric -CH_2 vibration appears at lower region of spectra than -CH_2 antisymmetric stretching. The -CH_2 symmetric stretching modes of vibration appeared among 2900 cm^{-1}- 3000 cm^{-1} however antisymmetric

stretching appeared among 3100 cm^{-1}- 3000 cm^{-1} due to strong bond strength (Srivastava et al 2014). The intense polarized peak seems at 2994 cm^{-1}, 2977 cm^{-1} with significant intensity which is due to antisymmetric stretching however at lower wave numbers area two adjacent symmetric stretching modes seems at 2933 cm^{-1}, 2808 cm^{-1}. The in-plane bending scissoring -CH_2 modes appears at 1442 cm^{-1} 1443 cm^{-1} with significant intensity. Two back to back sharp peaks with significant intensity seems at 1367 cm^{-1},1369 cm^{-1} due to rocking of -CH_2. At very low frequencies twisting of -CH_2 along with several mixing band appears with significant frequencies.

-O-H modes of Vibration

The O–H stretching modes of vibration are seem in calculations. In most of studied -OH stretching vibration appears among 3700 cm^{-1}-3800 cm^{-1} (Sathyanarayana et al 2004). In our calculation -OH stretching vibration seems at 2478 cm^{-1}. In lower frequency region some mixing band along with -OH bending modes appears between 1817cm^{-1} and 1564cm^{-1}.

-C=O modes of vibration

The modes of stretching vibration appears due to vibration of both C and O atom with equal amplitude so shown significant intensity. In stretching modes of vibration in -C=O appears at lower frequency region 1388 cm^{-1} with significantly high intensity.

-C=C modes of vibrations

The semi-circle stretching known as C-C aromatic stretch are lies in between 1332 cm^{-1} to 1650 cm^{-1}. At lower wave numbers CC in plane bending modes appears with significant intensity. At lower frequency region some out of plane CCC bending modes which is described in such a way that every carbon of sextant going up out of the plane while intervening carbon of sextant going down of plane are appears also supported by literature.

Biological Activity and Docking Properties

Firstly, we have discussed several transport properties of one unit 4-phenyl piperazine by using ALOGPS2.1 program (Jorgensen et al 2000) which is depend on electro topological indices e.g. Log P and Log S. The appraised Log P (1.54) and Log S (-1.08) recommend that the 4-phenyl piperazine can travel in cell membranes. The computed Log S value lies within -1 to -6 lies within range of 85% drugs. Some biological activity of 4-phenyl piperazine are computed by using PASS software. The PASS forecasts 900 pharmacological properties with help of molecular mechanisms (Tetko et al 2001). The forecast of biological activity by PASS server created on structure-activity dealings (SAR). The cogency of based on accuracy of in prediction of biological activities of 46,000 drugs accuracy with 85% whose bioactivities are experimentally resolute.

The calculated biological activities of 4-phenyl piperazine by using PASS online server and are listed in Table-4. The 4-phenyl piperazine displays good activities against 5 Hydroxy tryptamine release stimulants (0.905), Antineurotic (0.837), Phobic disorders treatment (0.835), Nicotinic alpha6beta3beta4alpha5 receptor antagonist (0.830), 27-Hydroxycholesterol 7alpha-monooxygenase inhibitor (0.762), Kidney function stimulant (0.719) etc.

The docking of 4-phenyl piperazine with 5B8U protein has been performed by using Auto Dock 4.2 software. In this process grid of 60 Å × 60 Å × 60 Å size was designated for docking. The swiss dock online server predict target protein. For this SIMILI code of optimized geometry of 4-phenyl piperazine is uploaded on site. The Swiss dock predict 5B8U protein for docking. The X-ray crystallographic structures of antiviral agent 5B8U were taken from protein databank (https ://www.rcsb.org/) with protein ID 5B8U. In docking process, first we prepare co-crystallized bonding coordinate and H_2O molecules were removed from the selected Protein Data Bank (PDB file) (https://www.rcsb.org/structure). The bond orders were allotted, and likely absent

hydrogen atoms in the PBD structure. Complete energetic optimization was achieved in the last modification phase utilizing OPLS3 force field. The Discovery Studio software used for visualization of interactions of 4-phenyl piperazine with 5B8U protein.

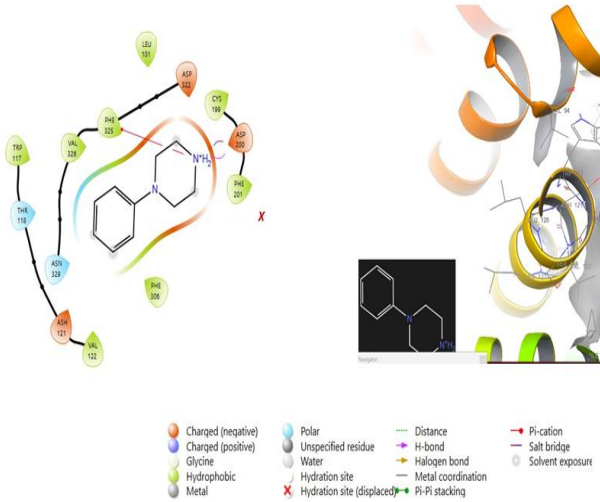

Fig-6 Molecular Docking picture of 5B8U protein with 4-(4-nitrophenyl) piperazin-1-ium

Table-4 Calculated Biology activity of 4(4-nitrophenyl) piperazin-1-ium for Pa>70%

S N.	Biological Activity	Pa	Pi
1	5 Hydroxytryptamine release stimulant	0.905	0.005
2	anti-inflammatory	0.889	0.006
3	Antineurotic	0.837	0.011
4	Nicotinic alpha6beta3beta4alpha5 receptor antagonist	0.830	0.007
5	Phobic disorders treatment	0.835	0.021
6	Anxiolytic	0.787	0.005
7	27-Hydroxycholesterol 7alpha-monooxygenase inhibitor	0.762	0.008
8	Mucomembranous protector	0.756	0.033
9	Kidney function stimulant	0.719	0.007
10	Polyamine-transporting ATPase inhibitor	0.712	0.011
11	Fusarinine-C ornithinesterase inhibitor	0.717	0.019

The docking procedures use numerous counting purposes to assess the binding affinity of the ligand-receptor complex. In docking process for energy with each possible conformation of ligand is computed. The computed full fitness (FF) score binding affinity is then utilize binding strength of 4-phenyl piperazine with 5B8U protein. The docking of 4-phenyl piperazine with 5B8U shown in figure-6. In this docking figure one H-bond appears in between nitrogen (NH_2 group) with residue PHE126 having bond length 2.45A^0. The computed full fitness score (732.43a.u.) and binding affinity (ΔGr=-6.28kcal/mol) shows that 4-phenyl) piperazine well dock with 5B8U protein.

Conclusion

In present communication the geometry optimization of 4-phenyl piperazin-1-ium trifluoroacetate salt has been done by using combination of DFT/B3LYP method and 6-

311G(d,p) basis set. The QTAIM analysis shows that a nonbonding interaction appears in between O_{26}-H_{27} which also confirm by NBO analysis. In salt formation charge transfer from 4-phenyl piperazin-1-ium to trifluoroacetate species stabilised its electrovalent nature. The vibrational analysis also confirms this nonbonding interaction by large polarity arise during -C=O stretching vibration with red shifted vibration. The electronic reactivity parameters show that reactivity falls in organic molecular range. Due to appearance of piperazine ring large polarity arise due to presence of two N atoms on opposite site of hetrocyclic ring shows good transport properties e.g. large Log P and Log S. The piperazine shows good activity against anti-inflammatory(0.889), Antineurotic (0.837), Phobic disorders treatment (0.835) activity, so to design new anti-inflammatory drug. The docking Full fitness score, binding affinity of 4-phenyl piperazine with 5B8U protein established that 4-phenyl piperazine bind well with 5B8U protein. The whole calculation performed on monomer in gas phase so ignore various effects arises in solvent bulk phase.

Acknowledgment

One of the authors, Anoop Kumar Pandey is grateful to Uttar Pradesh government (India) [No:46/2021/603/sattar-4-2021-4(56)/2020] for financial assistance.

References

Bose S C, Saleem H, Erdogdu Y, Rajarajan G, Thanikachalam V (2011). FT-Raman, FT-IR spectra and total energy distribution of 3-pentyl-2,6-diphenylpiperidin-4-one: DFT method. Spectrochim. Acta, A82: 260.

Chattaraj P K, Giri S (2007). Stability, Reactivity, and Aromaticity of Compounds of a Multivalent Superatom. J. Phys. Chem. A 111, 11116-11121.

Colthup N B, Daly L H, Wiberley S E (1990). Introduction to infrared and Raman spectroscopy. 3rd Ed. Boston, MA: Academic Press.

Dennington R, Keith T A, Millam J M (2016). Gauss View Version 6.1, Semichem Inc., Shawnee Missi.

Dwivedi A, Pandey A K, Mishra N (2012). Comparative Study of Vibrational spectra of two well known natural products Lupeol and Lupenone Using Density Functional Theory. Spectroscopy: An International Journal, Volume27, Issue 3, Pages155–166

Espinosa E, Molins E, and Lecomte C (1998). Chem. Phys. Lett., 285, 170-173.

Faist J, Seebacher W, Saf R, Brun R, Kaiser M, Weis R (2012). Eur. J. Med. Chem., 47(1), 510-519

Frisch M J et al (2009). Gaussian 09; Gaussian Inc. Pittsburgh, PA.

Ghorbani Mohammed Ali, Bushra B A, Zabiulla M S V, Shaukath A K (2015). Piperazine and morpholine: Synthetic preview and pharmaceutical applications. J chem pharm res. ; 7(5):281-301.

Gutsev G L, Weatherford C A, Johnson L E, Jena P (2012). Structure and properties of the aluminium borates Al $(BO2)_n$ (n= 1–4), J. Comput. Chem. 33 (4), 416–424.

Hohenberg P, Kohn W, Inhomogeneous Electron Gas. Phys. Rev B,1964136, 13864.

Jorgensen W L, Duffy E M (2000). Prediction of drug solubility from Monte Carlo simulations,Bioorg. Med. Chem. Lett., 10, 1155.

Kharb R, Sharma P C, Bhandari A, Shaharyar M (2012). Synthesis, spectral characterization and anthelmintic evaluation of some novel imidazole bearing triazole derivatives. Der Pharmacia Lettre, 4(2), 652-657.

Kharb R, Sharma P C, Shaharyar M (2011). New Insights into Chemistry and Anti-Infective Potential of Triazole Scaffold. Curr. Med. Chem., 18, 3265-3297.

Kharb R, Sharma P C, Shaharyar M (2011). Vistas on antimicrobial potential of novel oxadiazole derivatives in

modern medicinal chemistry. Mini Reviews Med. Chem., 11, 84-96.

Kharb R, Sharma P C, Shaharyar M, Enzyme J (2011). Hydrophilic Nonwoven Nanofiber Membranes as Nanostructured Supports for Enzyme Immobilization. Inhib. Med. Chem., 26(1), 1-21.

Kleinmann D A (1962). Nonlinear Dielectric Polarization in Optical Media. Phys. Rev., 126, 1977-1979.

Koch U, Popelier P (1995). Characterization of C-H-O Hydrogen Bonds on the Basis of the Charge Density. J. Phys. Chem., A 99, 9747-9754.

Kulig K, Sapa J, Maciag D, Filipek B, Malawska B (2007). Synthesis and Pharmacological Evaluation of New 1-[3-(4-Arylpiperazin-1-yl)-2-hydroxypropyl]-pyrrolidin-2-one Derivatives with Anti-arrhythmic, Hypotensive, and α-Adrenolytic Activity. Arch. Pharm., 340(9), 466-475.

Lee A Flippin, David W Gallagher, Keyvan Jalali-Araghi (1989). A convenient method for the reduction of ozonides to alcohols with borane-dimethyl sulfide complex. J. Org. Chem. 54, 1430-1432.

Lee C, Yang W T, Parr R G (1988). Development of the collesalvetti correlation-energy formula into a functional of electron density. Phys. Rev., 37, 785–789, https://doi.org/10.1103/physrevb.37.785

Lopez-Rodriguez M L, Ayala D, Benhamu B, Morcillo M J, Viso A (2002). Arylpiperazine derivatives acting at 5-HT(1A) receptors. Curr Med Chem. ;9:443-469;

Matta I F, and Boyd R J (2007). The Quantum Theory of Atoms in Molecules: From Solid State to DNA and Drug Design. Wiley-VCH Verlag Gmbh.

Murray J S, Sen K (1996). "Molecular electrostatic potentials, Concepts and Applications", Elsevier, Amsterdam.

Padmanabhan J, Parthasarathi R, Subramaniaan V, Chattaraj P K (2007). Electrophilicity-Based Charge.

Padrón J A, Carasco R, Pellón R F (2002). Molecular descriptor based on a molar refractivity partition using Randic-type graph-theoretical invariant J. Pharm. Pharmaceut. Sci. 5, 258–266.

Palwasha Khan , Tariq Mahmood , Khurshid Ayub , Sobia Tabassum , Mazhar Amj ad Gilani (October 2021). Turning diamondoids into nonlinear optical materials by alkali metal Substitution: A DFT investigation Optics & Laser TechnologyVolume 142, 107231.

Pandey A K, Siddiqui S A, Mishra N (2013). Comparative study of vibrational spectra of two narcotic compounds using Density Functional Theory. ChineseJournalofPhysicsVOL.51,NO. 3.

Pandey A K, Shukla S, Yadav O P, Singh V, Dwivedi A (2024). A Computational Quantum Chemical Approach for Surface Assimilation Effects of Well-Known Voltage Sensitive Potassium Channel Blockers (4-Aminopyridine and 3,4-Diaminopyridine) over Carbon Nanotube. Macromol. Symp., 413, 2300083DOI: 10.1002/masy.202300083.

Pandey Anoop Kumar, Singh Vijay, Pandey Kamal Kumar, Dwivedi Apoorva Kumar , Chauhan Madan Singh, Sharma Dipendra (2023). Influence of electric field on the electro-optical and electronic properties of 4-n-alkoxy-4′-cyanobiphenyl liquid crystal series: An ab initio study. Pramana –Journal of Physics Pramana–J. Phys. (2023) 97:93

Parr R G, Szentpály L V, Liu S (1999). Electrophilicity Index. J. Am. Chem. Soc. 121, 1922-1924.

Patel R V, Park S W (2013). An evolving role of piperazine moieties in drug design and discovery. Mini Rev Med Chem. ;13(11):1579-1601. * This review summarizes the importance of Piperazine template in drug design and discovery targeting multiple biological sites.

Pietrzycka A, Stepniewski M, Waszkielewicz A M, Marona H (2006). Preliminary evaluation of antioxidant activity of some 1-(phenoxyethyl)-piperazine derivatives. Acta Pol. Pharm., 63(1), 19-24.

Prasad H J S, Devaraju A, Murthy S M, Kaspiaruk H, Yathirajan C H S, Foroe S and Checinska L (2023). Syntheses, crystal structures and Hirshfeld surface analysis of 4-(4-nitrophenyl) piperazin-1-ium trifluoroacetate and 4-(4-nitrophenyl) piperazin-1- ium trichloro acetate Acta Cryst., E79, 1–7.

Pulay P, Fogarasi G, Pongor G, Boggs J E, and Vargha A (1983). Combination of theoretical ab- initio and experimental information to obtain reliable harmonic force constants. Scaled quantum mechanical (QM) force fields for glyoxal, acrolein, butadiene, formaldehyde, and ethylene, J. Am. Chem. Soc. 105, pp. 7037–7047.

Rastogi V K, Palafox M A, Tanwar R P, Mittal L (2002). 3, 5-Difluorobenzonitrile: ab initio calculations, FTIR and Raman spectra. Spectrochim. Acta A 58 1987-2004.

Rozas I, Alkorta I, Elguero J (2000). Behavior of Ylides Containing N, O, and C Atoms as Hydrogen Bond Acceptors. J. Am. Chem. Soc., 122, 11154.

Sathyanarayana D N (2004) Vibrational Spectroscopy-Theory and Applications. New Age International (P) Limited Publishers, NewDelhi.

Scott A P and Random L (1996). Harmonic vibrational frequencies: An evaluation of Hartree–Fock, Møller–Plesset, quadratic configuration interaction, density functional theory, and semiempirical scale factors, J. Phys. Chem. 100, pp. 16502–16513.

Singh V, Diwedi A, tiwari A, Pandey A K (2024). A quantum chemical study on the enormously large nonlinear optical response of doped endohedral super alkali Na2F and super halogens MF4 (M=B, Al) with CNT(C56H16) cage, Macromol. Symp., 413, 2300085 DOI: 10.1002/masy.202300085.

Soskic V, Joksimovic J (1998). Bioisosteric approach in the design of new dopaminergic/serotonergic ligands. Curr Med Chem. ;5:493-512.

Srivastava A, Pandey A K, Narayana B, Sarojini B K and Misra N (2014). Normal modes, Molecular Orbitals and Thermochemical analyses of 2, 4 anad 3, 4 dichloro substituted phenyl-N-(1, 3-thiazol-2-yl)acetamides: DFT Study and FTIR spectra, by Journal of Theoretical Chemistry Volume, Article ID125841, 10 pages ISNN 1082-4928.

Srivastava A K (2021). Lithiated Graphene Quantum Dot and its Nonlinear Optical Properties Modulated by a Single Alkali Atom: A Theoretical Perspective Inorg. Chem., 60, 3131−3138

Tetko I V, Tanchuk V Y, Kasheva T N, Villa A E P (2001). Internet software for the calculation of the lipophilicity and aqueous solubility of chemical compounds. J. Chem. Inf. Comput. Sci., 41, 246.doi:10.1021/ci00039.

Verma R P, Hansch C (2005). A comparison between two polarizability parameters in chemical- biological interactions. Bioorg. Med. Chem. 13,2355-2372.